

---

# PixelCNN Models with Auxiliary Variables for Natural Image Modeling

---

Alexander Kolesnikov<sup>1</sup> Christoph H. Lampert<sup>1</sup>

## Abstract

We study probabilistic models of natural images and extend the autoregressive family of PixelCNN architectures by incorporating auxiliary variables. Subsequently, we describe two new generative image models that exploit different image transformations as auxiliary variables: a quantized grayscale view of the image or a multi-resolution image pyramid. The proposed models tackle two known shortcomings of existing PixelCNN models: 1) their tendency to focus on low-level image details, while largely ignoring high-level image information, such as object shapes, and 2) their computationally costly procedure for image sampling. We experimentally demonstrate benefits of the proposed models, in particular showing that they produce much more realistically looking image samples than previous state-of-the-art probabilistic models.

## 1. Introduction

Natural images are the main input to visual processing systems and, thus, understanding their structure is important for building strong and accurate automatic vision systems. Image modeling is also useful for a wide variety of key computer vision tasks, such as visual representation learning, image inpainting, deblurring, super-resolution, image compression, and others.

Natural image modeling is known to be a very challenging statistical problem. Because the distribution over natural images is highly complex, developing models that are both accurate and computationally tractable is very challenging. Until recently, most of the existing models were restricted to modeling very small image patches, no bigger than, e.g., 9x9 pixels. Recently, however, deep convolutional neural networks (CNNs) have triggered noticeable advances in probabilistic image modeling. Out of these, PixelCNN-

type models (van den Oord et al., 2016a;b; Salimans et al., 2017), have shown to deliver the best performance, while at the same time staying computationally tractable. However, PixelCNNs also have noticeable shortcomings: unless conditioned on external input, the samples they produce rarely reflect global structure of complex natural images, see (van den Oord et al., 2016b; Salimans et al., 2017). This raises concerns that current PixelCNN architectures might also be more limited than originally presumed. Moreover, PixelCNN’s image sampling procedure is relatively slow in practice, as it requires to invoke a very deep neural network for every single image pixel that is to be generated.

In this work we derive improved PixelCNN models that address several of the aforementioned shortcomings. The main idea is to augment PixelCNN with appropriate auxiliary variables in order to isolate and overcome these drawbacks. This step, at the same time, provides us with important insights into the task of modeling natural images.

Besides the above insight, we make two main technical contributions in this paper. First, we show that uncertainty in low-level image details, such as texture patterns, dominates the objective of ordinary probabilistic PixelCNN models and, thus, these models may have little incentive to capture visually essential high-level image information, such as object shapes. We tackle this issue by deriving *Grayscale PixelCNNs* that effectively decouple the tasks of modeling low and high-level image details. This results in image samples of substantially improved visual quality. Second, we show that the sampling speed of PixelCNN models can be largely accelerated. We accomplish this by deriving *Pyramid PixelCNNs* that decompose the modeling of the image pixel probabilities into a series of much simpler steps. Employing a much lighter-weight PixelCNN architecture for each of them, globally coherent high-resolution samples can be obtained at reduced computational cost.

## 2. Related Work

Probabilistic image modeling is a research area of long tradition that has attracted interest from many different disciplines (Ruderman & Bialek, 1994; Olshausen & Field, 1996; Hyvärinen et al., 2009). However, because of the difficulty of the problem, until recently all existing models were restricted to small image patches, typically between

<sup>1</sup>IST Austria, Klosterneuburg, Austria. Correspondence to: Alexander Kolesnikov <akolesnikov@ist.ac.at>.

3x3 and 9x9 pixels, and reflected only low-order statistics, such as edge frequency and orientation (Zhu et al., 1998; Roth & Black, 2005; Carlsson et al., 2008; Zoran & Weiss, 2011). Utilized as prior probabilities in combination with other probabilistic models, such as Markov random fields (Geman & Geman, 1984), these models proved to be useful for low-level imaging tasks, such as image denoising and inpainting. Their expressive power is limited, though, as one can see from the fact that samples from the modeled distribution do not resemble natural images, but rather structured noise.

This situation changed with the development of probabilistic image models based on deep neural networks, in particular variational auto-encoders (VAEs) and PixelCNNs. In this paper, we concentrate on the latter. The PixelCNN family of models (van den Oord et al., 2016a;b; Salimans et al., 2017) factorizes the distribution of a natural image using the elementary chain rule over pixels. The factors are modeled as deep convolutional neural networks with shared parameters and trained by maximum likelihood estimation.

VAEs (Kingma & Welling, 2014) offer an alternative approach to probabilistic image modeling. They rely on a variational inequality to bound the intractable true likelihood of an image by a tractable approximation. VAEs are efficient to evaluate, but so far, produce results slightly worse than state-of-the-art PixelCNNs, both the likelihood scores and sampled images. Recent advances (Gregor et al., 2015; 2016; Bachman, 2016; Kingma et al., 2016; Gulrajani et al., 2017; Chen et al., 2017) in VAEs literature exploit modifications of model structure, including usage of latent variables and autoregression principle, though these techniques remain technically and conceptually different from PixelCNNs.

Specifically for the task of producing images and other complex high-dimensional objects, *generative adversarial networks* (GANs) (Goodfellow et al., 2014) have recently gained popularity. In contrast to PixelCNNs and VAEs, GANs are not explicit probabilistic models but feed-forward networks that are directly trained to produce naturally looking images from random inputs. A drawback of GAN models is that they have a generally unstable training procedure, associated with the search of a Nash equilibrium between two competing network players, and they can suffer from various technical problems, such as mode collapse or vanishing gradients. In order to make GANs work in practice, researchers resort to multiple non-trivial heuristics (Salimans et al., 2016). This strongly contrasts with probabilistic autoregressive models, such as PixelCNNs, which rely on well understood likelihood maximization for training and do not suffer from mode collapse problems.

Despite having fundamental differences on the technical level, PixelCNNs, VAEs and GANs may also benefit each

other by sharing ideas. In particular, our work is related to the line of work on GANs with controllable image structure (Reed et al., 2016; Wang & Gupta, 2016). A crucial difference of our work is, however, that our models do not require external supervision and, thus, remain purely unsupervised. Another notable paper in the context of this work introduces Laplacian GANs (Denton et al., 2015), with which we share the similar idea of using multi-scale decomposition for image generation. Similar constructions were suggested in (van den Oord et al., 2016b) in the context of recurrent networks and (Dahl et al., 2017) for the problem of super-resolution.

Very recent work (Reed et al., 2017), which appeared in parallel with ours, also addresses PixelCNN’s sampling speed with multi-scale decomposition. Unlike our work, this paper makes strong additional independence assumption on the pixel level. Our paper makes a largely complementary contribution, as we explore different angles in which a multi-scale approach can improve performance.

### 3. PixelCNNs with Auxiliary Variables

In this section we remind the reader of the technical background and develop a framework for PixelCNNs with auxiliary variables. We then propose two new PixelCNN instances that provide insights into the natural image modeling task and lead to improved quality of sampled images and accelerated sampling procedure. Finally, we conclude the section with implementation and training details.

We define an image  $X = (x_1, x_2, \dots, x_n)$  as a collection of  $n$  random variables associated with some unknown probability measure  $p(X)$ . Each random variable represents a 3-channel pixel value in the RGB format, where each channel takes a discrete value from the set  $\{0, 1, 2, \dots, 255\}$ . The pixels are ordered according to a raster scan order: from left to right and from top to bottom. Given a dataset  $\mathcal{D}$  of  $N$  images, our main goal is to estimate the unknown probability measure  $p(X)$  from  $\mathcal{D}$ .

Recall that PixelCNNs are a family of models (van den Oord et al., 2016a;b; Salimans et al., 2017) that factorize the distribution of natural images using the basic chain rule:

$$p(X) = \prod_{j=1}^n p(x_j | x_1, \dots, x_{j-1}). \quad (1)$$

Our key idea is to introduce an additional auxiliary variable,  $\hat{X}$ , into the image modeling process. Formally, a PixelCNN with auxiliary variable is a probabilistic model of the joint distribution of  $X$  and  $\hat{X}$ , factorized as

$$p(X, \hat{X}) = p_{\hat{\theta}}(\hat{X})p_{\theta}(X|\hat{X}), \quad (2)$$

where  $[\theta, \hat{\theta}]$  are the model parameters. The conditional

probability distribution,  $p_\theta(X|\hat{X})$ , is modeled using the PixelCNN model (van den Oord et al., 2016b), including the recent improvements suggested in (Salimans et al., 2017):

$$p_\theta(X|\hat{X}) = \prod_{j=1}^n p_\theta(x_j|x_1, \dots, x_{j-1}; f_w(\hat{X})), \quad (3)$$

where  $f_w$  is an embedding function parametrized by a parameter vector  $w$ .

Like other PixelCNN-based models, our model can be used for drawing samples. For a fixed  $\hat{X}$ , one follows the ordinary PixelCNN’s sampling strategy. Otherwise, one first samples  $\hat{X}$  from  $p_{\hat{\theta}}(\hat{X})$  and then samples  $X$  from  $p_\theta(X|\hat{X})$  as described before. Specifically, in this work we concentrate on auxiliary variables that 1) are a form of images themselves such that we can model  $p_{\hat{\theta}}(\hat{X})$  by a PixelCNN-type model, and 2) for which  $\hat{X}$  is approximately computable by a known deterministic function  $\psi : X \rightarrow \hat{X}$ . This choice has the useful consequence that  $p(\hat{X}|X)$  is going to be a highly peaked distribution around the location  $\psi(X)$ , which provides us with a very efficient training procedure: denoting the model parameters  $\Theta = (\hat{\theta}, \theta, w)$ , we jointly maximize the log-likelihood of the observed training data  $\mathcal{D}$  and the corresponding auxiliary variables,  $\hat{X} = \psi(X)$ . More precisely, we solve

$$\begin{aligned} \Theta^* &= \operatorname{argmax}_{\Theta} \sum_{X \in \mathcal{D}} \log p(X, \hat{X}) \\ &= \operatorname{argmax}_{\Theta} \sum_{X \in \mathcal{D}} \log p_\theta(X|\psi(X)) + \sum_{X \in \mathcal{D}} \log p_{\hat{\theta}}(\psi(X)). \end{aligned} \quad (4)$$

Because the objective function decomposes and the parameters do not interact, we can perform the optimization over  $\hat{\theta}$  and  $(\theta, w)$  separately, and potentially in parallel.

Note, that by this procedure we maximize a lower bound on the log-likelihood of the data:

$$\log \prod_{X \in \mathcal{D}} p(X, \hat{X}) \leq \log \prod_{X \in \mathcal{D}} p(X) \quad (5)$$

By making the lower bound high we also guarantee that the log-likelihood of the data itself is high. Furthermore, we expect the bound (5) to be (almost) tight, as  $p(X, \hat{X}) = p(\hat{X}|X)p(X)$ , and by construction the first factor,  $p(\hat{X}|X)$  is (almost) a  $\delta$ -peak centered at  $\hat{X} = \psi(X)$ .

In the rest of this section we present two concrete realizations of the PixelCNNs augmented with auxiliary variables.

### 3.1. Grayscale PixelCNN

Despite great success of PixelCNN-type models, they are still far from producing plausible samples of complex natural scenes. A visual inspection of samples produced by the

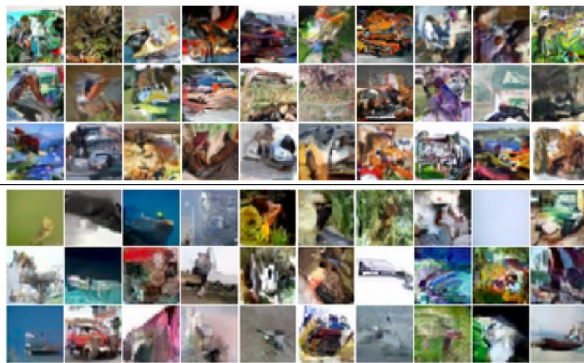


Figure 1. Samples produced by the current state-of-the-art autoregressive probabilistic image models: (van den Oord et al., 2016b) (top) and (Salimans et al., 2017) (bottom).

current state-of-the-art models reveals that they typically match low-level image details well, but fail at capturing global image structure, such as object shapes, see Figure 1 for an illustration.

We conjecture that a major reason for this is that the PixelCNN training objective provides too little incentive for the model to actually capture high-level image structure. Concretely, the PixelCNN’s loss function (the negative data log-likelihood) measures the amount of uncertainty of the color value of each pixel, conditioned on the previous ones. This quantity is dominated by hard-to-predict low-level cues, such as texture patterns, which exhibit a large uncertainty. As a consequence, the probabilistic model is encouraged to represent such textures well, while visually more essential image details, such as object shapes, are neglected. We provide quantitative evidence for this claim in our experimental section. Similar findings are also discussed in (Salimans et al., 2017).

In order to tackle the aforementioned shortcoming we derive *Grayscale PixelCNN*, in which the auxiliary variable  $\hat{X}$  is a 4-bit per pixel quantized grayscale version of the original 24-bits color image  $X$ . In combination with the factorization (2), this choice of auxiliary variable decouples the modeling of low and high-level image details: the distribution  $p_{\hat{\theta}}(\hat{X})$  (the quantized grayscale image) contains most information about global image properties, reflecting present objects and their shapes. The distribution  $p_\theta(X|\hat{X})$  models missing color and texture details. In Section 4 we highlight the quantitative and qualitative effects of augmenting PixelCNN with this choice of auxiliary variable.

### 3.2. Pyramid PixelCNN

In this section we address two further shortcomings of existing PixelCNN models. First, the strong asymmetry of the factors in Equation (1): the top left pixel of an image

is modeled unconditionally, i.e. without any available information, while the bottom right pixel has access to the information of, potentially, all other pixel values. Nevertheless, the same network is evaluated to model either of them (as well as all others pixels in between). We conjecture that it would be beneficial if pixels were generated with a less asymmetric usage of the image information.

Second, PixelCNNs have high computational cost for sampling images due to the recurrent nature of the procedure: for each generated pixel, the PixelCNN must invoke a convolutional neural network that is very deep, often in the order of a hundred convolutional layers. Note, that, in principle, at the sampling phase PixelCNN allows to cache intermediate values across consecutive PixelCNN invocations and, thus, save considerable computational effort. However, as reported in (Ramachandran et al., 2017), caching delivers minor sampling speed gain, when only a few or a single image is generated at once, which is a common scenario in real-life applications.

In order to alleviate the aforementioned drawbacks we propose a PixelCNN model in which the auxiliary variable  $\hat{X}$  corresponds to a twice lower resolution view of  $X$ , thereby decoupling the full image model into a pair of simpler models: creating a lower resolution image, and upscaling a low-res into a high-res image. The upscaling step has strongly reduced model asymmetry, because all pixels on the high scale have equal access to all information from the lower scale. Also, by explicitly modeling the low-resolution image view we make it easier for the model to capture long-range image correlations, simply because the “long range” now stretches over fewer pixels.

Since the proposed auxiliary variable is an ordinary image, we can recursively apply the same decomposition to model the auxiliary variable itself. For example, if we apply decomposition recursively 4 times for modeling 128x128 images, it will result in a model, which first generates an image on 8x8 resolution, and then upscales it 4 times by a factor 2. We call the resulting model *Pyramid PixelCNN*, as it resembles image pyramid decomposition.

*Pyramid PixelCNNs* break the image model into a series of simpler sub-models. Each sub-model is determined by the corresponding conditional distribution  $p_{\theta}(X|\hat{X})$  and the embedding  $f_w(\hat{X})$  (or just by  $p_{\hat{\theta}}(\hat{X})$  for the lowest resolution image). These conditional distributions model relatively simple task of producing an image, given an embedding of the slightly lower resolution view of this image. Thus, we hypothesize that with an appropriate embedding function (potentially modeled by a very deep network), the conditional distributions can be reliably modeled using a very light-weight network. We then expect a significant sampling speed acceleration, because the major part of computational burden is redistributed to the embed-

ding functions  $f_w(\hat{X})$ , which needs to be computed only once per pyramid layer, not once for each pixel.

We quantify the modeling performance and sampling speed of the proposed multi-scale model later in Section 4.

### 3.3. Details of model parameterization

The PixelCNN model with auxiliary variable is fully defined by factors in (2), each of which is realized by a network with the PixelCNN++ architecture. This is described in details in (Salimans et al., 2017). The output of the PixelCNN++ is a 10-component mixture of three-dimensional logistic distributions that is followed by a discretized likelihood function (Kingma et al., 2016; Salimans et al., 2017). The only exception is the model for 4-bit quantized grayscale auxiliary variable  $\hat{X}$ , where output is a vector of 16 probabilities for every possible grayscale value, followed by the standard cross-entropy loss.

The conditional PixelCNN model,  $p(X|\hat{X})$ , depends on auxiliary variable  $\hat{X}$  in a fashion similar to (van den Oord et al., 2016a; Salimans et al., 2017). It can be summarized in two steps as follows: compute an embedding of  $\hat{X}$  using a convolutional network  $f_w(\hat{X})$ , and bias the convolutions of every residual block by adding the computed embedding. We choose the architecture for modeling the embedding function,  $f_w(\hat{X})$ , to be almost identical to the architecture of PixelCNN++. The main difference is that we use only one flow of residual blocks and do not shift the convolutional layers outputs, because there is no need to impose sequential dependency structure on the pixel level.

For numeric optimization, we use Adam (Kingma & Ba, 2014), a variant of stochastic gradient optimization. During training we use dropout with 0.5 rate, in a way that suggested in (Salimans et al., 2017). No explicit regularization is used. Further implementation details, such as number of layers are specified later in Section 4.

## 4. Experiments

In this section we experimentally study the proposed *Grayscale PixelCNN* and *Pyramid PixelCNN* models on natural image modeling task and report quantitative and qualitative evaluation results.

### 4.1. Grayscale PixelCNN

**Experimental setup.** We evaluate the modeling performance of a *Grayscale PixelCNN* on the CIFAR-10 dataset (Krizhevsky & Hinton, 2009). It consists of 60,000 natural images of size  $32 \times 32$  belonging to 10 categories. The dataset is split into two parts: a training set with 50,000 images and a test set with 10,000 images. We augment the training data by random horizontal image flipping.

For setting up the architectures for modeling the distributions  $p_{\hat{\theta}}(\hat{X})$ ,  $p_{\theta}(X|\hat{X})$  and embedding  $f_w(X)$  we use the same hyperparameters as in (Salimans et al., 2017). The only exception is that for parameterizing  $p_{\theta}(X|\hat{X})$  and  $f_w(\hat{X})$  we use 24 residual blocks instead of 36.

In the Adam optimizer we use an initial learning rate of 0.001, a batch size of 64 images and an exponential learning rate decay of 0.99999 that is applied after each iteration. We train the grayscale model  $p_{\hat{\theta}}(\hat{X})$  for 30 epochs and the conditional model  $p_{\theta}(X|\hat{X})$  for 200 epochs.

**Modeling performance.** The *Grayscale PixelCNN* achieves an upper bound on the negative log-likelihood score of **2.98** bits-per-dimension. This is on par with current state-of-the-art models, see Table 1. Note, that since we measure an upper bound, the actual model performance might be slightly better. However, in light of our and other experiments, we believe small differences in this score to be of minor importance, as the log-likelihood does not seem to correlate well with visual quality in this regime.

In Figure 2 we present random samples produced by the *Grayscale PixelCNN* model, demonstrating grayscale samples from  $p_{\hat{\theta}}(\hat{X})$  and resulting colored samples from  $p_{\theta}(X|\hat{X})$ . We observe that the produced samples are highly diverse, and, unlike samples from previously proposed probabilistic autoregressive models, often exhibit a strongly coherent global structure, resembling highly complex objects, such as cars, dogs, horses, etc.

Given the high quality of the samples, one might be worried if possibly the grayscale model,  $p_{\hat{\theta}}(\hat{X})$ , had overfit the training data. We observe that training and test loss of  $p_{\hat{\theta}}(\hat{X})$  are very close to each other, namely 0.442 and 0.459 of bits-per-dimension, which speaks against significant overfitting. Note also, that it is not clear if an overfitted model would automatically produce good samples. For instance, as reported in (Salimans et al., 2017), severe overfitting of the PixelCNN++ model does not lead to a high perceptual quality of sampled images.

**Discussion.** By explicitly emphasizing the modeling of high-level image structures in the *Grayscale PixelCNN*, we achieve significantly better visual quality of the produced samples. Additionally, the *Grayscale PixelCNN* offers interesting insights into the image modeling task. As the objective we minimize for training is a sum of two scores, we can individually examine the performance of auxiliary variable model  $p(\hat{X})$  and the conditional model  $p(X|\hat{X})$ . The trained conditional model achieves  $p(X|\hat{X})$  a negative log-likelihood score of **2.52** bits-per-dimension, while  $p(\hat{X})$  achieves a score of **0.459** bits-per-dimension on the CIFAR-10 test set. In other words: high-level image properties, despite being harder to model for the network, contribute only a small fraction of the uncertainty score to the

Model	Bits per dim.
Deep Diffusion (Sohl-Dickstein et al., 2015)	$\leq 5.40$
NICE (Dinh et al., 2015)	4.48
DRAW (Gregor et al., 2015)	$\leq 4.13$
Deep GMMs (van den Oord & Schrauwen, 2014)	4.00
Conv Draw (Gregor et al., 2016)	$\leq 3.58$
Real NVP (Dinh et al., 2017)	3.49
Matnet + AR (Bachman, 2016)	$\leq 3.24$
PixelCNN (van den Oord et al., 2016b)	3.14
VAE with IAF (Kingma et al., 2016)	$\leq 3.11$
Gated PixelCNN (van den Oord et al., 2016a)	3.03
PixelRNN (van den Oord et al., 2016b)	3.00
<b>Grayscale PixelCNN</b> (this paper)	$\leq 2.98$
DenseNet VLAE (Chen et al., 2017)	$\leq 2.95$
PixelCNN++ (Salimans et al., 2017)	2.92

Table 1. The negative log-likelihood of the different models for the CIFAR-10 test set measured as bits-per-dimension.

the overall log-likelihood. We take this as indication that if low-level and high-level image details are modeled by one model, then at training time low-level image uncertainty will dominate the training objective. We believe that this is the key reason why previously proposed PixelCNN models failed to produce globally coherent samples of natural images. Importantly, this problem does not appear in the *Grayscale PixelCNN*, because global and local image models do not share parameters and, thus, do not interfere with each other at training phase.

An alternative explanation for the differences in log-likelihood scores would be that PixelCNN-type models are actually not very good at modeling low-level image input. Additional experiments that we performed show that this is not the case: we applied the learned conditional model  $p(X|\hat{X})$  to 4-bit grayscale images obtained by quantizing real images of the CIFAR-10 test set. Figure 3 compares the resulting colorized samples with the corresponding original images, showing that the samples produced by our conditional model are of visual quality comparable to the original images. This suggests that in order to produce even better image samples, mainly improved models for  $p_{\hat{\theta}}(\hat{X})$  are required.

## 4.2. Pyramid PixelCNN.

**Experimental setup.** We evaluate the *Pyramid PixelCNN* on the task of modeling face images. We rely on the *aligned&cropped CelebA* dataset (Liu et al., 2015) that contains approximately 200,000 images of size 218x178. In order to focus on human faces and not background, we preprocess all images in the dataset by applying a fixed 128x128 crop (left margin: 25 pixels, right margin: 25 pixel, top margin: 50, bottom margin: 40 pixels). We use a random 95% subset of all images as training set and the remaining images as a test set.



Figure 2. Random quantized grayscale samples from  $p(\hat{X})$  (top) and corresponding image samples from  $p(X|\hat{X})$  (bottom). The grayscale samples show several recognizable objects, which are subsequently also present in the color version.



Figure 3. CIFAR-10 images in original color (left) and quantized to 4-bit grayscale (center). Images sampled from our conditional model  $p(X|\hat{X})$ , using the grayscale CIFAR images as auxiliary variables (right). The images produced by our model are visually as plausible as the original ones.

Res.	8×8	16×16	32×32	64×64	128×128
Bpd	4.58	4.30	3.33	2.61	1.52

Table 2. Bits-per-dimension (*Bpd*) achieved by *Pyramid PixelCNN* on the test images from the *CelebA* dataset for various resolutions (*Res.*).

For the *Pyramid PixelCNN* we apply the auxiliary variable decomposition 4 times. This results in a sequences of probabilistic models, where the first model generates faces in 8×8 resolution. We use a PixelCNN++ architecture without down or up-sampling layers with only 3 residual blocks to model the distributions  $p_{\theta}(\hat{X})$  and  $p_{\hat{\theta}}(X|\hat{X})$  for all scales. For the embedding  $f_w(\hat{X})$  we use a PixelCNN++ architecture with 15 residual blocks with downsampling layer after the residual block number 3 and upsampling layers after the residual blocks number 9 and 12. For all convolutional layers we set the number of filters to 100.

In the Adam optimizer we use an initial learning rate 0.001, a batch size of 16 and a learning rate decay of 0.999995. We train the model for 60 epochs.

**Modeling performance.** We present a quantitative evaluation of *Pyramid PixelCNN* in Table 2. We evaluate the performance of our model on different output resolutions, observing that bits-per-dimension score is smaller for higher resolutions, as pixel values are more correlated and, thus, easier to predict. As an additional check, we also train and evaluate *Pyramid PixelCNN* model on the CIFAR dataset, achieving a competitive score of 3.32 bits-per-dimension.

Before demonstrating and discussing face samples produced by our model we make an observation regarding the PixelCNN’s sampling procedure. Recall that the output of the *Pyramid PixelCNN* is a mixture of logistic distributions. We observe an intriguing effect related to the mixture representation of the predicted pixel distributions for face images: the perceptual quality of sampled faces substantially increases if we artificially reduce the predicted variance of the mixture components. We illustrate this effect in Figure 4, where we alter the variance by subtracting constants from a fixed set of  $\{0.0, 0.1, \dots, 1.0\}$  from the predicted log-variance of the mixture components. Inspired by this observation we propose an alternative sampling procedure: for each pixel, we randomly sample one of the logistic components based on their weight in the predicted mixture. Then, we use the mode of this component as sampled pixel value, instead of performing a second random sampling step. This sampling procedure can be seen as a hybrid of probabilistic sampling and maximum a posteriori (MAP) prediction.

Figure 5 shows further samples obtained by such *MAP sampling*. The produced images have very high perceptual quality, with some generated faces appearing almost photo-

realistic. The complete multi-scale sampling mechanism of the *Pyramid PixelCNN*, from 8×8 to 128×128 images, is demonstrated in Figure 6.

**Discussion.** First, we observe that, despite the very high resolution of modeled images, the produced samples capture global human face characteristics, such as arrangement of face elements and global symmetries. At the same time, the set of samples is diverse, containing male as well as female faces, different hair and skin colors as well as facial expressions and head poses. Second, we emphasize that by properly decomposing the model we are able to scale the *Pyramid PixelCNN* to produce samples with very high resolution of 128x128. As discussed previously in Section 3, this results from the fact that our decomposition allows to parametrize autoregressive parts of the image model by a light-weight architecture. Concretely, on an NVidia TitanX GPU, our *Pyramid PixelCNN* without caching optimizations requires approximately **0.004** seconds on average to generate one image pixel, while a PixelCNN++ even with recently suggested caching optimizations requires roughly **0.05** seconds for the same task. If we add caching optimizations to our model, we expect its speed to improve even further.

## 5. Conclusion

In this paper we presented *Grayscale PixelCNN* and *Pyramid PixelCNN*, an improved autoregressive probabilistic techniques that incorporate auxiliary variables. We derived two generative image models that exploit different image views as auxiliary variables and address known limitations of existing PixelCNN models. The use of quantized grayscale images as auxiliary variables resulted in a model that captures global structure of complex natural images and produces globally coherent samples. With multi-scale image views as auxiliary variable, the model was able to efficiently produce realistic high-resolution images of human faces. Note, that these improvements are complementary and we plan to combine them in a future work.

Furthermore, we gained interesting insights into the image modeling problem. First, our experiments suggest that texture and other low-level image information distract probabilistic models from focusing on more essential high-level image information, such as object shapes. Thus, it is beneficial to decouple the modeling of low and high-level image details. Second, we demonstrate that multi-scale image model, even with very shallow PixelCNN architectures, can accurately model high-resolution face images.

**Acknowledgments.** We thank Tim Salimans for spotting a mistake in our preliminary *arXiv* manuscript. This work was funded by the European Research Council under the European Unions Seventh Framework Programme (FP7/2007-2013)/ERC grant agreement no 308036.

### PixelCNN Models with Auxiliary Variables for Natural Image Modeling

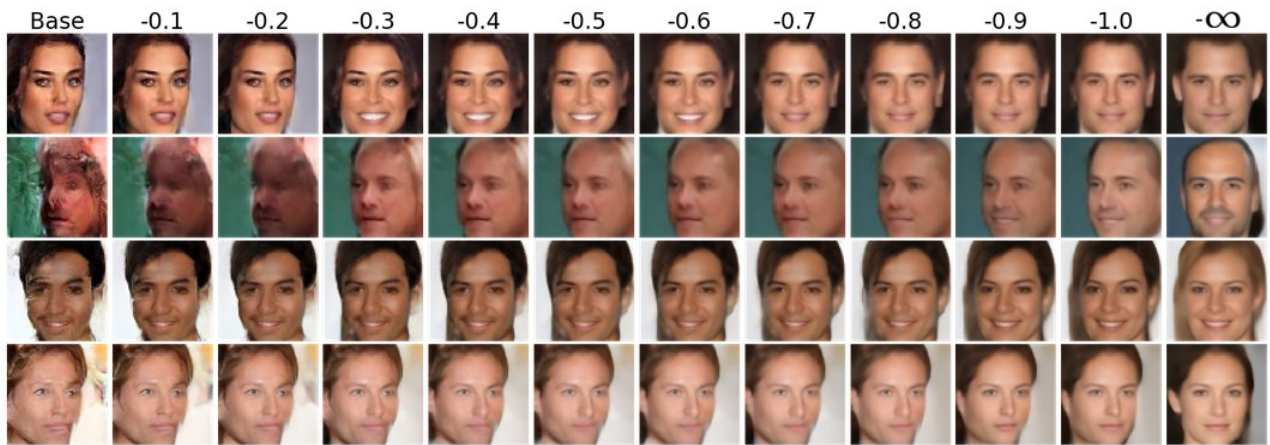


Figure 4. Effect of the variance reduction. Numbers on top of each column indicates the amount of reduction in the predicted log-variance of the mixture components. The last column corresponds to MAP sampling.

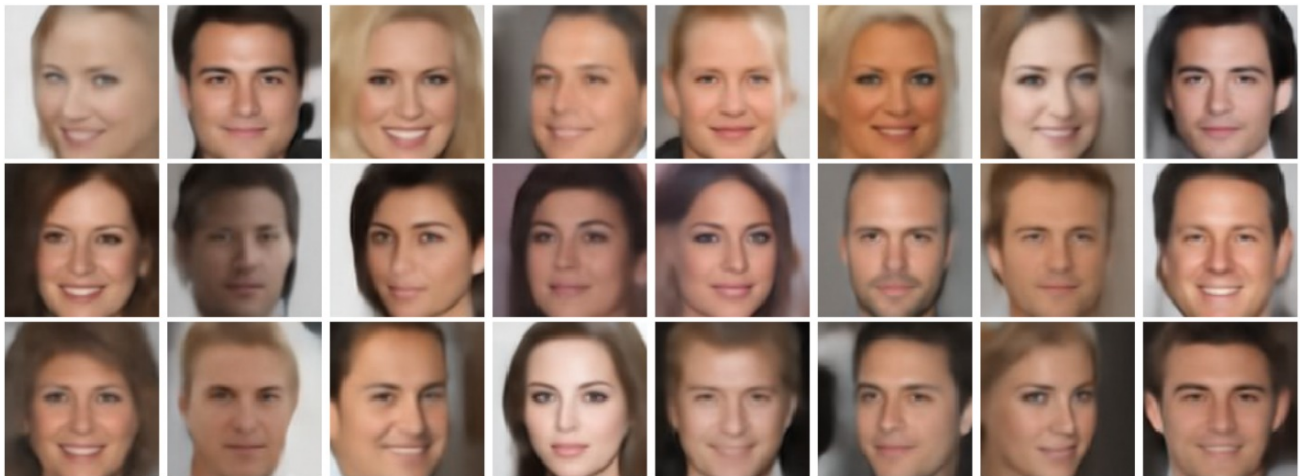


Figure 5. Images sampled from the *Pyramid PixelCNN* by MAP sampling. The generated faces are of very high quality, many being close to photorealistic. At the same time, the set of sample is diverse in terms of the depicted gender, skin color and head pose.

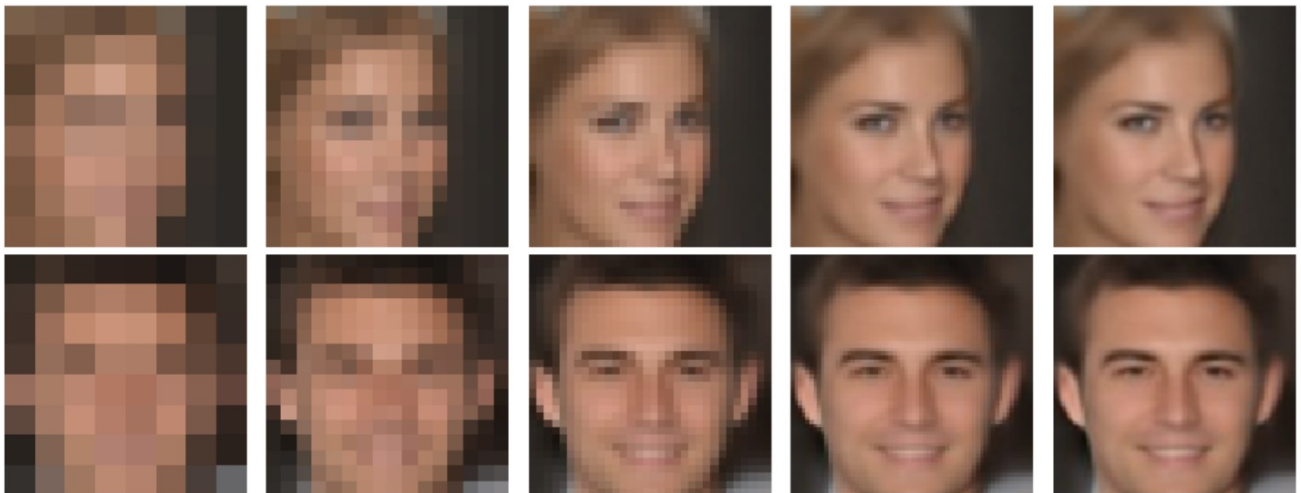


Figure 6. Visualization of the *Pyramid PixelCNN* sampling process. Faces are first generated on a small, 8x8, resolution and then are gradually upsampled until reaching the desired 128x128 resolution.



## References

- Bachman, Philip. An architecture for deep, hierarchical generative models. In *Conference on Neural Information Processing Systems (NIPS)*, 2016.
- Carlsson, Gunnar, Ishkhanov, Tigran, De Silva, Vin, and Zomorodian, Afra. On the local behavior of spaces of natural images. *International Journal of Computer Vision (IJCV)*, 76(1):1–12, 2008.
- Chen, Xi, Kingma, Diederik P, Salimans, Tim, Duan, Yan, Dhariwal, Prafulla, Schulman, John, Sutskever, Ilya, and Abbeel, Pieter. Variational lossy autoencoder. *International Conference on Learning Representations (ICLR)*, 2017.
- Dahl, Ryan, Norouzi, Mohammad, and Shlens, Jonathon. Pixel recursive super resolution. *arXiv preprint arXiv:1702.00783*, 2017.
- Denton, Emily L, Chintala, Soumith, Fergus, Rob, et al. Deep generative image models using a laplacian pyramid of adversarial networks. In *Conference on Neural Information Processing Systems (NIPS)*, 2015.
- Dinh, Laurent, Krueger, David, and Bengio, Yoshua. NICE: Non-linear independent components estimation. *Workshop on International Conference on Learning Representations (Workshop on ICLR)*, 2015.
- Dinh, Laurent, Sohl-Dickstein, Jascha, and Bengio, Samy. Density estimation using real NVP. *International Conference on Learning Representations (ICLR)*, 2017.
- Geman, Stuart and Geman, Donald. Stochastic relaxation, gibbs distributions, and the bayesian restoration of images. *IEEE Transactions on Pattern Analysis and Machine Intelligence (T-PAMI)*, 6(6):721–741, 1984.
- Goodfellow, Ian, Pouget-Abadie, Jean, Mirza, Mehdi, Xu, Bing, Warde-Farley, David, Ozair, Sherjil, Courville, Aaron, and Bengio, Yoshua. Generative adversarial networks. In *Conference on Neural Information Processing Systems (NIPS)*, 2014.
- Gregor, Karol, Danihelka, Ivo, Graves, Alex, Rezende, Danilo, and Wierstra, Daan. Draw: A recurrent neural network for image generation. In *International Conference on Machine Learning (ICML)*, 2015.
- Gregor, Karol, Besse, Frederic, Jimenez Rezende, Danilo, Danihelka, Ivo, and Wierstra, Daan. Towards conceptual compression. In *Conference on Neural Information Processing Systems (NIPS)*, 2016.
- Gulrajani, Ishaan, Kumar, Kundan, Ahmed, Faruk, Taiga, Adrien Ali, Visin, Francesco, Vazquez, David, and Courville, Aaron. PixelVAE: A latent variable model for natural images. *International Conference on Learning Representations (ICLR)*, 2017.
- Hyvärinen, Aapo, Hurri, Jarmo, and Hoyer, Patrick O. *Natural Image Statistics: A Probabilistic Approach to Early Computational Vision.*, volume 39. Springer, 2009.
- Kingma, Diederik P. and Ba, Jimmy. Adam: A method for stochastic optimization. In *International Conference on Learning Representations (ICLR)*, 2014.
- Kingma, Diederik P and Welling, Max. Auto-encoding variational bayes. In *International Conference on Learning Representations (ICLR)*, 2014.
- Kingma, Diederik P., Salimans, Tim, and Welling, Max. Improving variational inference with inverse autoregressive flow. *Conference on Neural Information Processing Systems (NIPS)*, 2016.
- Krizhevsky, Alex and Hinton, Geoffrey. Learning multiple layers of features from tiny images. *Technical report, University of Toronto*, 2009.
- Liu, Ziwei, Luo, Ping, Wang, Xiaogang, and Tang, Xiaoou. Deep learning face attributes in the wild. In *International Conference on Computer Vision (ICCV)*, 2015.
- Olshausen, Bruno A and Field, David J. Natural image statistics and efficient coding. *Network: computation in neural systems*, 7(2):333–339, 1996.
- Ramachandran, Prajit, Paine, Tom Le, Khorrami, Pooya, Babaeizadeh, Mohammad, Chang, Shiyu, Zhang, Yang, Hasegawa-Johnson, Mark, Campbell, Roy, and Huang, Thomas. Fast generation for convolutional autoregressive models. *Workshop on International Conference on Learning Representations (Workshop on ICLR)*, 2017.
- Reed, Scott, Oord, Aäron van den, Kalchbrenner, Nal, Colmenarejo, Sergio Gómez, Wang, Ziyu, Belov, Dan, and de Freitas, Nando. Parallel multiscale autoregressive density estimation. *International Conference on Machine Learning (ICML)*, 2017.
- Reed, Scott E, Akata, Zeynep, Mohan, Santosh, Tenka, Samuel, Schiele, Bernt, and Lee, Honglak. Learning what and where to draw. In *Conference on Neural Information Processing Systems (NIPS)*, 2016.
- Roth, Stefan and Black, Michael J. Fields of experts: A framework for learning image priors. In *Conference on Computer Vision and Pattern Recognition (CVPR)*, 2005.
- Ruderman, Daniel L and Bialek, William. Statistics of natural images: Scaling in the woods. *Physical review letters*, 73(6):814, 1994.

- Salimans, Tim, Goodfellow, Ian, Zaremba, Wojciech, Cheung, Vicki, Radford, Alec, and Chen, Xi. Improved techniques for training GANs. In *Conference on Neural Information Processing Systems (NIPS)*, 2016.
- Salimans, Tim, Karpathy, Andrej, Chen, Xi, Knigam, Diederik P., and Bulatov, Yaroslav. PixelCNN++: A PixelCNN implementation with discretized logistic mixture likelihood and other modifications. *International Conference on Learning Representations (ICLR)*, 2017.
- Sohl-Dickstein, Jascha, Weiss, Eric, Maheswaranathan, Niru, and Ganguli, Surya. Deep unsupervised learning using nonequilibrium thermodynamics. In *International Conference on Machine Learning (ICML)*, 2015.
- van den Oord, Aaron and Schrauwen, Benjamin. Factoring variations in natural images with deep gaussian mixture models. In *Conference on Neural Information Processing Systems (NIPS)*, 2014.
- van den Oord, Aaron, Kalchbrenner, Nal, Espeholt, Lasse, Vinyals, Oriol, and Graves, Alex. Conditional image generation with pixelCNN decoders. In *Conference on Neural Information Processing Systems (NIPS)*, 2016a.
- van den Oord, Aaron, Kalchbrenner, Nal, and Kavukcuoglu, Koray. Pixel recurrent neural networks. *International Conference on Machine Learning (ICML)*, 2016b.
- Wang, Xiaolong and Gupta, Abhinav. Generative image modeling using style and structure adversarial networks. In *European Conference on Computer Vision (ECCV)*, 2016.
- Zhu, Song Chun, Wu, Yingnian, and Mumford, David. Filters, random fields and maximum entropy (FRAME): Towards a unified theory for texture modeling. *International Journal of Computer Vision (IJCV)*, 27(2):107–126, 1998.
- Zoran, Daniel and Weiss, Yair. From learning models of natural image patches to whole image restoration. In *International Conference on Computer Vision (ICCV)*, 2011.